Theor Chem Acc (2012) 131:1199
DOI 10.1007/s00214-012-1199-6

REGULAR ARTICLE

The DFT investigations of the electron injection in hydrazone-based sensitizers

Abdullah G. Al-Sehemi · Ahmad Irfan · Abdullah M. Asiri

Received: 17 January 2012 / Accepted: 27 February 2012 / Published online: 14 March 2012

Abstract Quantum chemical calculations were carried out by using density functional theory and time-dependant density functional theory at B3LYP/6-31G(d) and TD-B3LYP/6-31G(d) level of theories. The absorption spectra have been computed with and without solvent. The calculated absorption spectra in ethanol, acetonitrile, and methanol are in good agreement with experimental evidences. The absorption spectra are red shifted compared to System1. On the basis of electron injection and electronic coupling constant, we have shed light on the nature of different sensitizers. The coplanarity between the benzene near anchoring group having LUMO and the bridge (N–N) is broken in System6 and System7 that would hamper the recombination process. The electron injection of System2–System10 is superior to System1. The highest electronic coupling constant has been observed for System6 that followed the System7 and System8. The light-harvesting efficiency of all the sensitizers enlarged in acetonitrile and ethanol. The long-range-corrected functional (LC-BLYP), Coulomb-attenuating method (CAM-B3LYP), and BH and HLYP functional underestimate the excitation energies while B3LYP is good to reproduce the experimental data. Moreover, we have investigated the effect of cyanoacetic acid as anchoring group on the electron injection.

Keywords Dye-sensitized solar cells · Density functional theory · Time-dependant density functional theory · Absorption · Electron injection

1 Introduction

Dye-sensitized solar cells (DSSCs) are currently attracting widespread academic and commercial interest for the conversion of sunlight into electricity because of their low cost and high efficiency [1–6]. The basic design of today's high performance DSSCs was developed in the early 1990 by Grätzel et al. [7, 8]. The photoactive part of these devices consists of a wide-band-gap semiconductor covered by a monolayer of sensitizing dye. The semiconductor is directly supported by a transparent electrode on one side while dye is connected to the back electrode via a liquid electrolyte or a solid hole conducting material. The initial step of the photovoltaic process is light-induced electron injection from the dye into the semiconductor material. This process yields an oxidized dye and an energetic electron. Ruthenium-based sensitizers, such as N3 [9], N719 [10], and black dye [11], have achieved good efficiencies. Efficiencies surpassing the N3-based standard cells were also reported [12, 13]. There is increasing interest in metal-free organic sensitizers because of the rarity and high cost of the ruthenium metal. Moreover, high

Electronic supplementary material The online version of this article (doi:10.1007/s00214-012-1199-6) contains supplementary material, which is available to authorized users.

A. G. Al-Sehemi · A. Irfan (✉)
Chemistry Department, Faculty of Science,
King Khalid University, Abha, Saudi Arabia
e-mail: irfaahmad@gmail.com

A. G. Al-Sehemi
e-mail: agmasq@gmail.com

A. M. Asiri
Chemistry Department, Faculty of Science,
King Abdulaziz University, P.O. Box 80203,
Jeddah 21589, Saudi Arabia

A. M. Asiri
Center of Excellence for Advanced Materials Research,
King Abdulaziz University, P.O. Box 80203,
Jeddah 21589, Saudi Arabia

molar extinction coefficients of metal-free organic dyes allow the use of thinner TiO_2 films, which is beneficial for charge separation. Efficiencies of 9% have been achieved for DSSCs using metal-free sensitizers [14, 15]. Very high conversion efficiency (10%) and excellent stability was also reported in a recent paper of Wang [16]. The development of highly efficient light-harvesting systems remains a challenging task as many aspects need improvement like the choice of the chromophores, linker types, and connection sites.

Numerous efficient organic dyes for DSSCs, such as hemicyanine-, polyene-, thienylfluorene-, phenothiazine-, merocyanine-, coumarin-, and indoline-based organic dyes, have been developed and showed good DSSCs performance [17–22]. In this regard, enormous studies have been focused on energy-level engineering of chromophores to attain a capability of panchromatic light harvesting [23, 24]. Several groups focused on the electronic structures and absorption properties of dye sensitizers [25–34].

Donor–acceptor metal-free organic dyes showed promising properties [35–37]. Recently, we have synthesized different hydrazone-based sensitizers (System1–System10) [38, 39], see scheme 1. The intramolecular charge transfer (ICT) process plays a vital role in achieving higher efficiency, and electron transfer (ET) remains passionate topic of research. The ICT and ET will be investigated by means of theoretical investigations. To elucidate the experimental evidences, quantum mechanical techniques are efficient. The time-dependent density functional theory (TDDFT) will be used for the electronic excited states calculations. The electronic coupling between the reactants and the products (*V*RP) will been investigated. Moreover, in the last section, we will shed light on the absorption, electron coupling, electron injection, and light-harvesting efficiency of new designed sensitizer (System11) where cyanoacetic acid has been substituted as anchoring group. Then, we will compare the electron injection of COOH containing dyes to the other sensitizer. By using density functional theory (DFT) and TDDFT, we have shed light on the absorption, electron coupling constant, light-harvesting efficiency (LHE), and electron injection. We have also discussed the structure–property relationship.

2 Computational details

Stein et al. studied the charge-transfer excitations in a series of coumarin-based donor-bridge-acceptor dyes. They explained that excitation energies well reproduced by using a range-separated hybrid functional within the generalized Kohn–Sham approach to TDDFT [40]. The absorption and fluorescence properties in a class of oligothiophene push–pull biomarkers have been investigated with a long-range-corrected (LC) density functional method [41]. The excited-state properties in a series of coumarin solar cell dyes were investigated with LC-BLYP [42]. The range-separation technique is based on a more physical model of the exchange potential. The B3LYP hybrid functional underestimates vertical excitation energies, especially for larger dye molecules. The B3LYP calculations showed good agreement for the small C343 and NKX-2388 dyes [42]. It has been already reported that the choice of the range-separation parameter is strongly system dependent [43–46]. The long-range "Coulomb-attenuating method" (CAM-B3LYP) has been applied to investigate the excitation energies for TPA-based dyes [47]. In all these investigated systems, organic sensitizers consisted electron donor and acceptor separated from each other by conjugated units. Tretiak and Magyar demonstrated that a good description of the CT states can be achieved when a large fraction of HF exchange is used [49]. Preat et al. suggested that the percentage of the HF (exact) exchange is crucial and the estimated absorption wavelength decreases when increasing the amount of HF exchange incorporated in the functional [48]. Moreover, in our recent study, we have demonstrated that BH and HLYP is good to reproduce the excitation energies for TPA-based sensitizers [50, 51]. The "LC" functionals are more efficient in many cases [52] but sometime underestimate the absorption spectra for small molecules. Therefore, the use of conventional DFT approaches to compute auxochromic shifts for CT dyes remains usual [53, 54].

Guillaumont and Nakamura calculated the maximum absorption wavelength of several organic dyes (indigo, azobenzene, phenylamine, hydrazone, and anthraquinone) with an average deviation close to 0.20 eV. Moreover, B3LYP functional reproduces the experimental absorption wavelength very well for hydrazone-based dye with an average deviation 0.12 eV [55].

It is clearly stated that LC functionals are good to reproduce the excitation energies for donor-bridge-acceptor (large molecules). Moreover, Wong and Cordaro showed that B3LYP is good choice for small molecules [42]. Thus, we have computed the excitation energies of hydrazone-based dyes by using B3LYP functional, which are small molecules and the charge separation is not in the long range from donor to acceptor like TPA- and coumarin-based dyes [40–42, 47, 48]. The iodine/iodide couple is used as regenerator in DSSCs, implying that the solar cells work in solvent phase. Thus, UV/Vis data for dyes are reported in solvent. Additionally, we have also computed the excitation energies of System7 that is more efficient by using long-rang corrected functionals (LC-BLYP and CAM-B3LYP) and BH and HLYP by using time-dependant density functional theory in methanol (polarizable continuum model (PCM) was used). We found that BH and HLYP,

Scheme 1 Schematic diagram of investigated sensitizers from System1–System10

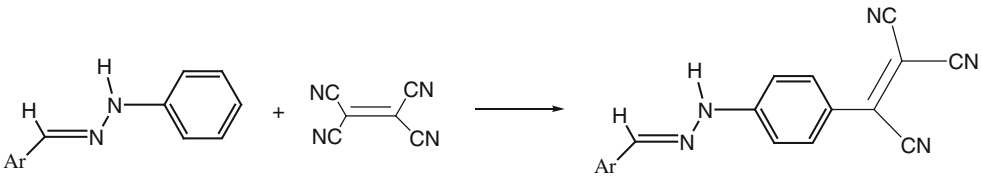

System No.	Structures	System No.	Structures
System1	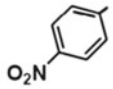	System6	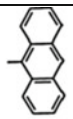
System2	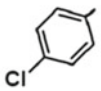	System7	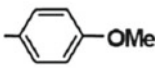
System3	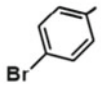	System8	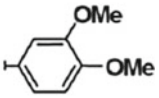
System4		System9	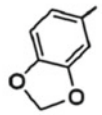
System5		System10	

LC-BLYP, and CAM-B3LYP underestimate the absorption wavelengths for System7, that is, 83, 135, and 79 nm, respectively. We observed that B3LYP (PCM, methanol) is better, accurate, and reasonable choice than BH and HLYP, LC-BLYP, and CAM-B3LYP (PCM, methanol) to reproduce the experimental data (see Table 1).

The molecular structures of all the dyes have been optimized using DFT calculations with B3LYP/6-31G(d) level of theory [56–60]. The TD-DFT has been applied to compute the absorption spectra at the TD-B3LYP/6-31G(d) level of theory that has been proved accurate and reliable method [61–65]. All of the calculations were performed by using Gaussian-09 program package [66]. The polarizable continuum model (PCM) [67–70] is used for evaluating bulk solvent effects at all stages. The PCM-TDB3LYP/6-31G(d) level is used to explain the charge transfer (CT). The calculations have been carried out in ethanol, methanol, and acetonitrile solvents.

The description of the electron transfer from a dye to a semiconductor and the rate of the charge transfer process can be derived from the general classical Marcus theory [71–74],

$$k_{inject} = |V_{RP}|(2/h\ (\pi/\lambda k_B T)1/2 \times \exp\left[-\left(\Delta G^{inject} + \lambda\right)2/4\lambda k_B T\right] \quad (1)$$

In Eq. 1, k_{inject} is the rate constant (in S^{-1}) of the electron injection from dye to TiO_2, k_B is the Boltzmann thermal energy, h the Planck constant, $-\Delta G^{inject}$ is the free energy of injection, λ is the reorganization energy of the system, and $|V_{RP}|$ is the coupling constant between the reagent and the product potential curves. Eq. 1 revealed that larger $|V_{RP}|$ leads to higher rate constant that would result better sensitizer. The use of the generalized Mulliken–Hush formalism (GMH) allows evaluating |VRP| for a photoinduced charge transfer [72, 73]. The Hsu et al. [73] explained that |VRP| can be evaluated as

Table 1 Calculated absorption wavelengths (λ_a) in nm of System1–System10

Systems	Assignments	λ_a^a	λ_a^b	λ_a^c	λ_a^d	λ_a^e
System1	H→L	527	528	528	465	512
System2	H→L	536	537	537	476	523
System3	H→L	538	539	539	479	522
System4	H→L	534	535	535	473	522
System5	H→L	590	591	591	519	528
System6	H-1→L	500	500	500	473[i]	535
System7	H→L	578	579	580	506	541
	H→L	458[f]				
	H→L	406[g]				
	H→L	462[h]				
System8	H→L	580	581	581	508	544
System9	H→L	602	603	603	520	
System10	H→L	560	561	561	491	

[a] λ_a in methanol
[b] λ_a in acetonitrile
[c] λ_a in ethanol
[d] λ_a in gas phase
[e] λ_a = experimental data; excitation from (H→L) HOMO to LU MO and (H-1→L) HOMO-1 to LUMO
[f] PCM-TDBH and HLYP
[g] PCM-TDLC-BLYP
[h] PCM-TDCAM-B3LYP
[i] HOMO to LUMO+1

$$|\mathrm{VRP}| = \Delta E_{\mathrm{RP}}/2 \tag{2}$$

The injection driving force can be formally expressed within Koopmans approximation as

$$\Delta E_{\mathrm{RP}} = \left[E_{\mathrm{LUMO}}^{\mathrm{dye}} + 2E_{\mathrm{HOMO}}^{\mathrm{dye}}\right] - \left[E_{\mathrm{LUMO}}^{\mathrm{dye}} + E_{\mathrm{HOMO}}^{\mathrm{dye}} + E_{\mathrm{CB}}^{\mathrm{TiO_2}}\right] \tag{3}$$

where $E_{\mathrm{CB}}^{\mathrm{TiO_2}}$ conduction band edge. Though it is often difficult to accurately determine $E_{\mathrm{CB}}^{\mathrm{TiO_2}}$, because it is highly sensitive to the conditions, for example, the pH of the solution, thus we used $E_{\mathrm{CB}}^{\mathrm{TiO_2}} = -4.0$ eV [75], which is experimental value corresponding to conditions where the semiconductor is in contact with aqueous redox electrolytes of fixed pH 7.0 [76, 77].

More quantitatively for a closed-shell system $E_{\mathrm{LUMO}}^{\mathrm{dye}}$ corresponds to the reduction potential of the dye $\left(E_{\mathrm{RED}}^{\mathrm{dye}}\right)$, whereas the HOMO energy is related to the potential of first oxidation (i.e., $-E_{\mathrm{HOMO}}^{\mathrm{dye}} = E_{\mathrm{OX}}^{\mathrm{dye}}$). As a result, Eq. 3 becomes

$$\Delta E_{\mathrm{RP}} = \left[E_{\mathrm{HOMO}}^{\mathrm{dye}} - E_{\mathrm{OX}}^{\mathrm{dye}}\right] = -\left[E_{\mathrm{OX}}^{\mathrm{dye}} + E_{\mathrm{CB}}^{\mathrm{TiO_2}}\right] \tag{4}$$

The Eq. 4 can be rewritten as

$$\Delta E_{\mathrm{RP}} = E_{0-0}^{\mathrm{dye}} - \left[2E_{\mathrm{CB}}^{\mathrm{TiO_2}} + E_{\mathrm{RED}}^{\mathrm{dye}} + E_{\mathrm{CB}}^{\mathrm{TiO_2}}\right] \tag{5}$$

The free energy change (eV) for the electron injection can be expressed as [76],

$$\Delta G^{\mathrm{inject}} = E_{\mathrm{OX}}^{\mathrm{dye}*} - E_{\mathrm{CB}}^{\mathrm{TiO_2}} \tag{6}$$

where $E_{\mathrm{OX}}^{\mathrm{dye}*}$ is the oxidation potential of the dye in the excited state, and $E_{\mathrm{CB}}^{\mathrm{TiO_2}}$ is the reduction potential of the semiconductor conduction band. Two models can be used for the evaluation of $E_{\mathrm{OX}}^{\mathrm{dye}*}$ [78]. The first implies that the electron injection occurs from the unrelaxed excited state. For this reaction path, the excited-state oxidation potential can be extracted from the redox potential of the ground state, $E_{\mathrm{OX}}^{\mathrm{dye}}$, which has been calculated at the PCM-B3LYP-6-31G(d) approach and the vertical transition energy corresponding to the photoinduced intramolecular CT (ICT),

$$E_{\mathrm{OX}}^{\mathrm{dye}*} = E_{\mathrm{OX}}^{\mathrm{dye}} - \lambda_{\mathrm{max}}^{\mathrm{ICT}} \tag{7}$$

where $\lambda_{\mathrm{max}}^{\mathrm{ICT}}$ is the energy of the ICT. Note that this relation is only valid if the entropy change during the light absorption process can be neglected. For the second model, one assumes that electron injection occurs after relaxation. Given this condition, $E_{\mathrm{OX}}^{\mathrm{dye}*}$ is expressed as [31]:

$$E_{\mathrm{OX}}^{\mathrm{dye}*} = E_{\mathrm{OX}}^{\mathrm{dye}} - E_{0-0}^{\mathrm{dye}} \tag{8}$$

where E_{0-0}^{dye} is the 0–0 transition energy between the ground state and the excited state. To estimate the 0–0 "absorption" line, we need both the S_0 (singlet ground state) and the S_1 (first singlet excited state) equilibrium geometries, Q_{S0} and Q_{S1}, respectively:

$$E_{0-0} = E_{S0}(Q_{S0}) - E_{S1}(Q_{S1}). \tag{9}$$

Preat et al. concluded that the absolute difference between the relaxed and unrelaxed $\Delta G^{\mathrm{inject}}$ is constant and is of the same order of magnitude than the $E_{\mathrm{OX}}^{\mathrm{dye}}$ and $E_{\mathrm{OX}}^{\mathrm{dye}*}$ [47, 48]. Here, $\Delta G^{\mathrm{inject}}$ and $E_{\mathrm{OX}}^{\mathrm{dye}*}$ have been evaluated using Eqs. 6 and 7.

The light-harvesting efficiency (LHE) of the dye has to be as high as possible to maximize the photocurrent response. Here, LHE is expressed as [79]:

$$\mathrm{LHE} = 1 - 10^{-A} = 1 - 10^{-f} \tag{10}$$

where A (f) is the absorption (oscillator strength) of the dye associated with the $\lambda_{\mathrm{max}}^{\mathrm{ICT}}$. The oscillator strength is directly derived from the TDDFT calculations and writes:

$$f = \frac{2}{3}\lambda_{max}^{ICT}|\vec{\mu}0 - ICT|^2 \quad (11)$$

where μ0–ICT is the dipolar transition moment associated with the electronic excitation. In order to maximize f, both λ_{max}^{ICT} and μ0–ICT must be large [80, 81].

3 Results and discussion

3.1 Absorption

In Table 1, we have presented the computed absorption spectra of System1–System10 in methanol, ethanol, and acetonitrile. We have compared the absorption spectra of System1 with other investigated sensitizers. By replacing the nitro group with chloro, we have observed red shift in the absorption spectra in acetonitrile and methanol ca. 9 nm in both the solvents. The bromo substitution at the same position is also red shifted ca. 11 nm in acetonitrile and methanol. But the absorption spectra for System2 and System3 are almost same which revealed that bromo has no momentous consequence than chloro. The System4 where benzyl group has been substituted as donor is 7 nm red shifted while System5 is 63 nm red shifted in both the solvents. In System6, anthryl is at donor side, which is 27 and 28 nm blue shifted in acetonitrile and methanol, respectively. The System7 and System8 are 51 and 53 nm red shifted compared to the System1. System9 and System10 are red shifted ca. 75 and 33 nm, respectively. The computed absorption spectra are in good agreement with the experimental evidence. The computed absorption spectra in methanol of all the investigated sensitizers are similar to the calculated absorption spectra in acetonitrile and ethanol.

The absorption spectra of investigated sensitizers have been computed at the same level of theory without considering the solvent. We have observed that all of the investigated dyes (System2–System10) are red shifted ca. 11, 14, 8, 54, 8, 41, 43, 55, and 26 nm, respectively, compared to System1. From Table 1, it can be seen that the solvents are good to reproduce the experimental absorption spectra except for System5, which is overestimated. On other hand, the absorption spectra without solvent at the same level of theory is underestimated except for System5 that is in good agreement with experimental evidence. It can be seen that the assignments for absorption are HOMO to LUMO except for System6 that has assignment HOMO−1 to LUMO in the solvents while HOMO to LUMO+1 without solvent. Furthermore, we have computed the absorption wavelengths/excitation energies of System7 in methanol by using the long-range-corrected (LC) functionals. The LC-BLYP and CAM-B3LYP underestimate the absorption spectra 135 and 79 nm, respectively, compared to the experimental data. The BH and HLYP functional also underestimate the absorption spectra (83 nm). The BH and HLYP is better than LC functionals for the hydrazone-based sensitizer but inferior than B3LYP (see supporting information). It is expected that hydrazone-based sensitizers are small molecules so B3LYP is better choice for hydrazone-based sensitizers.

3.2 Electron injection

We have presented the ΔG^{inject}, E_{OX}^{dye}, E_{OX}^{dye*}, λ_{max}^{ICT}, LHE, |VRP|, and ΔG_r^{inject} in Table 2. It can be seen that electron injection boosts up from System1 to System2 by replacing nitro with chloro. Similarly, substituting bromo in place of nitro also enhanced the electron injection. The ΔG^{inject} (ΔG_r^{inject}) increases from −0.39 (0.195) to −0.53 (0.265) by replacing the nitro group with chloro (System2) or bromo (System3) at the same position, respectively. This is might be due to the reason that nitro is more electron withdrawing that is not favorable to promote the electron injection from donor to acceptor side. This statement can be verified by surveying the distribution pattern of HOMOs and LUMOs of the System1–System3. In System2 and Sytem3, the clear charge transfer has been observed from donor to acceptor side while in System1 charge is delocalized at nitro group and nearest benzene ring (donor side) as well. In System4, ΔG^{inject} and ΔG_r^{inject} augmented compared to System1–System3. It is might be due to that in System 4 there is no electron withdrawing group e.g. Cl, Br, and NO_2 like System1–System3 thus the ability from donor side to acceptor side has been enhanced leading towards boost up the electron injection. But the effect is not so significant. Similarly, the substitution of naphthyl (System5) also not improved the electron injection. We have explained the recombination barrier on the basis of distortion and coplanarity. The coplanarity between the benzene near anchoring group having LUMO and the bridge (N–N) is broken in System6, that is, 2.4° out-of-plane distortion; thus, the positive charge may not be directly in drop a line to the TiO_2 surface, consequently hampering the recombination reaction. Might be due to this reason, the electron injection in System6 is highest compared to other Systems. The mono- and di-methoxy substituted at benzene ring improve the donor ability. The ΔG^{inject} of System7 and System8 reaches to −0.61 that is higher than other studied sensitizers except System6 which revealed that these sensitizers (System7 and System8) would be more efficient than System1–System5, System9, and System10. But when we have look on the distortion, it has been observed that the coplanarity between the benzene near anchoring group having LUMO and the bridge (N–N)

Table 2 The ΔG^{inject}, oxidation potential, light-harvesting efficiency, |VRP| of investigated dyes at TD-B3LYP/6-31G(d) and PCM-B3LYP/6-31G(d) level of theory

System	ΔG^{inject}	$E_{\text{OX}}^{\text{dye}}$	$E_{\text{OX}}^{\text{dye}*}$	$\lambda_{\text{max}}^{\text{ICT}}$	f	LHE	$\Delta G_r^{\text{inject}}$	|VRP|
In methanol								
System1	−0.39	5.96	3.61	2.35	1.3189	0.9520	1.00	0.195
System2	−0.53	5.78	3.47	2.31	1.1011	0.9208	1.36	0.265
System3	−0.53	5.77	3.47	2.30	1.1060	0.9217	1.36	0.265
System4	−0.58	5.74	3.42	2.32	1.0726	0.9154	1.49	0.290
System5	−0.53	5.57	3.47	2.10	0.8800	0.8682	1.36	0.265
System6	−1.08	5.40	2.92	2.48	0.559	0.7239	2.73	0.540
System7	−0.61	5.53	3.39	2.14	0.9998	0.9000	1.56	0.305
System8	−0.61	5.53	3.39	2.14	0.9751	0.8941	1.56	0.305
System9	−0.58	5.48	3.42	2.06	0.7881	0.8371	1.49	0.290
System10	−0.58	5.63	3.42	2.21	1.0069	0.9016	1.49	0.290
In ethanol								
System1	−0.38	5.97	3.62	2.35	1.3265	0.9528	1.00	0.190
System2	−0.53	5.78	3.47	2.31	1.1096	0.9223	1.39	0.265
System3	−0.52	5.78	3.48	2.30	1.1146	0.9232	1.37	0.260
System4	−0.58	5.74	3.42	2.32	1.0811	0.9170	1.53	0.290
System5	−0.53	5.57	3.47	2.10	0.8906	0.8713	1.39	0.265
System6	−1.08	5.40	2.92	2.48	0.5563	0.7222	2.84	0.540
System7	−0.61	5.53	3.39	2.14	1.0094	0.9021	1.60	0.305
System8	−0.60	5.53	3.40	2.13	0.9852	0.8965	1.58	0.300
System9	−0.58	5.48	3.42	2.06	0.7995	0.8413	1.53	0.290
System10	−0.58	5.63	3.42	2.21	1.0163	0.9037	1.53	0.290
In acetonitrile								
System1	−0.39	5.96	3.61	2.35	1.3233	0.9525	1.00	0.195
System2	−0.55	5.76	3.45	2.31	1.1058	0.9216	1.41	0.275
System3	−0.53	5.77	3.47	2.30	1.1108	0.9225	1.36	0.265
System4	−0.58	5.74	3.42	2.32	1.0773	0.9163	1.49	0.290
System5	−0.53	5.57	3.47	2.10	0.8857	0.8699	1.36	0.265
System6	−1.08	5.40	2.92	2.48	0.5563	0.7222	2.73	0.540
System7	−0.61	5.53	3.39	2.14	1.0050	0.9011	1.56	0.305
System8	−0.60	5.53	3.40	2.13	0.9806	0.8954	1.54	0.300
System9	−0.57	5.48	3.43	2.05	0.7937	0.8392	1.46	0.285
System10	−0.58	5.63	3.42	2.21	1.0120	0.9027	1.49	0.290

ΔG_r^{inject} relative electron injection ΔG^{inject} (dye)/ΔG^{inject} (System1)

is broken in System7; thus, mono-methoxy-substituted system is more distorted accordingly impede the recombination process while di-methoxy-substituted system is coplanar which revealed that System7 would be more efficient than System8. In System9, benzo[1, 3]dioxo has been substituted, which leads ΔG^{inject} to −0.58 and $\Delta G_r^{\text{inject}}$ 0.29 revealed that benzo[1, 3]dioxo has no significant effect to enhancing the electron injection compared to benzyl substituted one (System4) while noteworthy effect has been observed toward the enhancement of electron injection compared to System1. In System10, the thiophene has been substituted in place of benzene that has also no considerable effect compared to System4. The ΔG^{inject} is −0.58 and $\Delta G_r^{\text{inject}}$ is 0.29, which is equal to System4. The electron injection of System2–System10 is superior to System1. The similar effect has been observed for electronic coupling constant (|VRP|); the highest |VRP| has been observed for System6 that followed the System7 and System8. The System6 has the highest electron injection and electronic coupling constant while smallest LHE (0.7239) compared to other sensitizers. The LHE of System7 and System8 is higher than System6. Generally, the electron injection of System2–System5, System9, and System10 is almost same which revealed that there would be no significant enhancement in the efficiency by changing the substituent from chlorobenzene to thiophene. The System6–System8 might be better sensitizers especially System6 and System7, which can hamper the recombination and improve the efficiency. If we compare System6 and System7 by considering the LHE then it can be

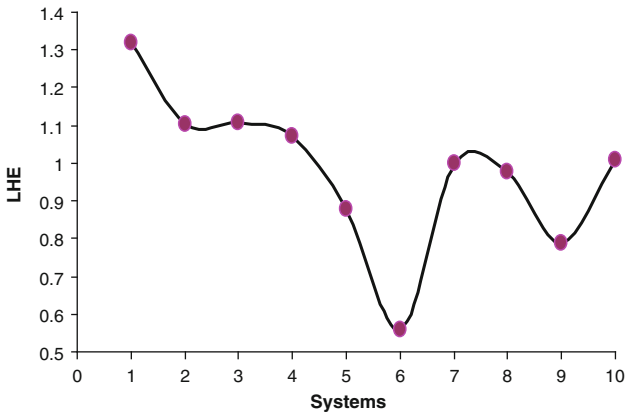

Fig. 1 The graph between light-harvesting efficiency (LHE) along *Y* axis and investigated systems in methanol along *X* axis

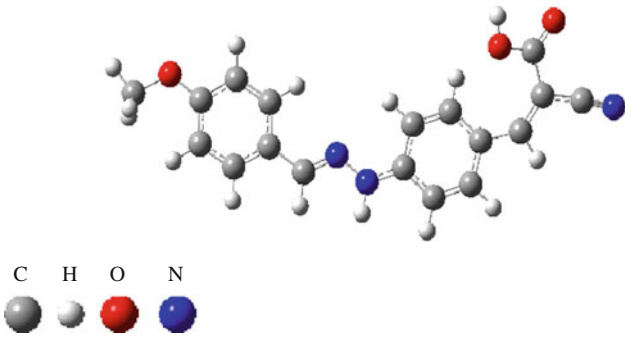

Fig. 2 The optimized structure of System11 with the atom *colors*

Table 3 Calculated absorption wavelengths (λ_a) in nm and ΔG^{inject}, oxidation potential, light-harvesting efficiency, |VRP| of investigated dyes at TD-B3LYP/6-31G(d) and PCM-B3LYP/6-31G(d) level of theory of System**11**

Parameters		Parameters	
Assignments	H→L	λ_{max}^{ICT}	2.72
λ_a	456	*f*	1.2538
ΔG^{inject}	−1.40	LHE	0.9442
E_{OX}^{dye}	5.32	|VRP|	0.70
E_{OX}^{dye*}	2.60		

[a] The methanol solvent has been used; excitation from (H→L) HOMO to LU MO

predicted that System7 would be better because System6 has the smallest LHE, see Fig. 1. Moreover, System7 is red shifted compared to System6. By comparing the System7 and System8, obviously, System7 would be better sensitizer that would hamper the recombination process.

Generally, ΔG_r^{inject} enhanced in ethanol for all of the studied Systems. As we mentioned above, mono-methoxy would be superior to di-methoxy that further corroborated from the electron injection behavior of System7 and System8 in ethanol. From Table 2, we found that ΔG_r^{inject} for System7 is 1.60 that is higher than System8, that is, 1.58 in ethanol. Moreover, LHE of System7 is higher than the System8, which revealed that System7 would be better sensitizer. The LHE of investigated sensitizers in ethanol is better than methanol.

It has been observed that ΔG^{inject} and |VRP| increased to −0.55 and 0.275 in acetonitrile compared to −0.53 and 0.265 in methanol and ethanol in System2, respectively. The ΔG_r^{inject} diminished in System8 compared to System7 from methanol to acetonitrile or ethanol. Even the effect is not so significant but it revealed that di-methoxy is more solvent dependant. Similar effect has been observed for System9 that showed drop off ΔG_r^{inject} in acetonitrile while improved in ethanol, but the progress of ΔG^{inject} is almost negligible. We have noticed that LHE of all the investigated sensitizers enlarged in acetonitrile except System6 in which it decline compared to methanol. Recently, we have synthesized these systems and fabricated. The highest efficiency has been observed for System7 ca. 0.37%. All other sensitizers have efficiency 0.19–0.27% for all the cases except for System6 that showed 0.16% efficiency [38, 39]. Our predicted results are verified by these experimental facts. The electron injection of System7 at BH and HLYP, LC-BLYP, and CAM-B3LYP functionals can be found in supporting information. Here, we did not explain the electron injection because these functionals underestimate the excitation energies that would mislead the electron injection behavior.

3.3 The effect of cyanoacetic acid on electron injection

We have checked the effect of cyanoacetic acid moiety as anchoring group on the electron injection. For this purpose, we have designed a new sensitizer (System11) from System7. In the new system, the CN have been deleted and the cyanoacetic acid moiety was substituted as electron acceptor that is good choice to improve the efficiency [82, 83], see Fig. 2. The absorption spectra of System11 is 456 nm that is 122 nm blue shifted compared to its counterpart System7. We have observed that substituting the cyanoacetic acid as anchoring group improves not only the LHE but also the electron injection. The electron coupling constant is also superior to System7 that revealed that the new designed sensitizer might be efficient than System7 (Table 3).

4 Conclusions

The long-range-corrected functionals underestimate the excitation energies while B3LYP is good to reproduce the experimental data. The computed absorption spectra in

methanol and ethanol of all the investigated sensitizers are similar to the calculated absorption spectra in acetonitrile. The TD calculations in solvents are in good agreement with the experimental evidence. Generally, computed absorption spectra are red shifted compared to System1 that is accordance with experiment. The nitro group is more electron-withdrawing group and is not favorable to promote the electron injection from donor to acceptor. In System4, ΔG^{inject} and $\Delta G_{\text{r}}^{\text{inject}}$ improved compared to System1–System3. The coplanarity between the benzene near anchoring group having LUMO and the bridge (N–N) is broken in System7, that is, 2.4°out-of-plane distortion; thus, the positive charge may not be directly in drop a line to the TiO_2 surface, consequently hampering the recombination reaction. The ΔG^{inject} and |VRP| of System7 and System8 are higher than other sensitizers except System6 that revealed that these sensitizers would be more efficient. System7 might be superior to System8 due to the distortion of the coplanarity, which would impede the recombination process. The LHE of System7 is higher than System6. Generally, the electron injection of System2–System5, System9, and System10 is almost same, which revealed that there would be no significant enhancement in the efficiency. We have noticed that LHE of all the investigated sensitizers enlarged in ethanol and acetonitrile. The LHE, electron coupling constant and electron injection of System11 is superior to System7.

Acknowledgments The present work has been carried out under project No. 08-NAN155-7 funded by KAUST (King Abdulaziz City for Science and Technology) through the Long Term Comprehensive National Plan for Science, Technology and Innovation program.

References

1. Fabregat-Santiago F, Garcia-Canadas J, Palomares E, Clifford JN, Haque SA, Durrant JR, Garcia-Belmonte G, Bisquert J (2004) The origin of slow electron recombination processes in dye-sensitized solar cells with alumina barrier coatings. J Appl Phys 96:6903–6907
2. Figgemeier E, Hagfeldt A (2004) Are dye-sensitized nanostructured solar cells stable? An overview of device testing and component analyses. Int J Photoenergy 6:127–140
3. Furube A, Katoh R, Yoshihara T, Hara K, Murata S, Arakawa H, Tachiya M (2004) Ultrafast direct and indirect electron-injection processes in a photoexcited dye-sensitized nanocrystalline zinc oxide film: the importance of exciplex intermediates at the surface. J Phys Chem B 108:12583–12592
4. Hongwei H, Xingzhong Z, Jian L (2005) Enhancement in photoelectric conversion properties of the dye-sensitized nanocrystalline solar cells based on the hybrid TiO_2 electrode. J Electrochem Soc 152:A164–A166
5. Kim JH, Kang M-S, Kim YJ, Won J, Park N-G, Kang YS (2004) Dye-sensitized nanocrystalline solar cells based on composite polymer electrolytes containing fumed silica nanoparticles. Chem Commun 1662–1663
6. Miyasaka T, Kijitori Y (2004) Low-temperature fabrication of dye-sensitized plastic electrodes by electrophoretic preparation of mesoporous TiO_2 layers. J Electrochem Soc 151:A1767–A1773
7. O'Reagan B, Grätzel M (1991) A low-cost, high-efficiency solar cell based on dyesensitized colloidal TiO_2 films. Nature 353:737–740
8. Grätzel M (2001) Photoelectrochemical cells. Nature 414:338–344
9. Grätzel M (2004) Corrigendum to "Conversion of sunlight to electric power by nanocrystalline dye-sensitized solar cells". J Photochem Photobiol, A 168:235
10. Nazeeruddin MK, Kay A, Rodicio L, Humphry-Baker R, Muller E, Liska P, Vlachopoulos N, Grätzel M (1993) Conversion of light to electricity by cis-X2bis(2,2′-bipyridyl-4,4′-dicarboxylate)ruthenium(II) charge-transfer sensitizers (X = Cl-, Br-, I-, CN-, and SCN-) on nanocrystalline titanium dioxide electrodes. J Am Chem Soc 115:6382–6390
11. Nazeeruddin MK, Pe′chy P, Renouard T, Zakeeruddin SM, Humphry-Baker R, Comte P, Liska P, Cevey L, Costa E, Shklover V, Spiccia L, Deacon GB, Bignozzi CA, Grätzel M (2001) Engineering of efficient panchromatic sensitizers for nanocrystalline TiO_2-based solar cells. J Am Chem Soc 123:1613–1624
12. Chen C-Y, Wu S-J, Li J-Y, Wu C-G, Chen J-G, Ho K-C (2007) A new route to enhance the light-harvesting capability of ruthenium complexes for dye-sensitized solar cells. Adv Mater 19:3888–3891
13. Chen C-Y, Chen J-G, Wu S-J, Li J-Y, Wu C-G, Ho K-C (2008) Multifunctionalized ruthenium-based super sensitizers for highly efficient dye-sensitized solar cells. Angew Chem Int Ed 47:7342–7345
14. Ito S, Zakeeruddin M, Hummphrey-Baker R, Liska P, Charvet R, Comte P, Nazeeruddin MK, Pe′chy P, Takata M, Miura H, Uchida S, Gratzel M (2006) High-efficiency organic-dye-sensitized solar cells controlled by nanocrystalline-TiO_2 electrode thickness. Adv Mater 18:1202–1205
15. Choi H, Baik C, Kang SO, Ko J, Kang M-S, Nazeeruddin MK, Grätzel M (2008) Highly efficient and thermally stable organic sensitizers for solvent-free dye-sensitized solar cells. Angew Chem Int Ed 47:327–330
16. Zhang G, Bala H, Cheng Y, Shi D, Lv X, Yu Q, Wang P (2009) High efficiency and stable dye-sensitized solar cells with an organic chromophore featuring a binary π-conjugated spacer. Chem Commun 2198–2200
17. Wang Z-S, Li F-Y, Huang C-H (2001) Photocurrent enhancement of hemicyanine dyes containing RSO_3-group through treating TiO_2 films with hydrochloric acid. J Phys Chem B 105:9210–9217
18. Thomas KRJ, Lin JT, Hsu Y-C, Ho K-C (2005) Organic dyes containing thienylfluorene conjugation for solar cells. Chem Commun 4098–4100
19. Tian H, Yang X, Chen R, Pan Y, Li L, Hagfeldt A, Sun L (2007) Phenothiazine derivatives for efficient organic dye-sensitized solar cells. Chem Commun 3741–3743
20. Li S-L, Jiang K-J, Shao K-F, Yang L-M (2006) Novel organic dyes for efficient dye-sensitized solar cells. Chem Commun 2792–2794
21. Wang Z-S, Cui Y, Dan-oh Y, Kasada C, Shinpo A, Hara K (2007) Thiophene-functionalized coumarin dye for efficient dye-sensitized solar cells: electron lifetime improved by coadsorption of deoxycholic acid. J Phys Chem C 111:7224–7230
22. Ito S, Miura H, Uchida S, Takata M, Sumioka K, Liska P, Comte P, Pechy P, Gratzel M (2008) High-conversion-efficiency organic dye-sensitized solar cells with a novel indoline dye. Chem Commun 5194–5196
23. Hara K, Kurashige M, Dan-oh Y, Kasada C, Shinpo A, Suga S, Sayama K, Arakawa H (2003) Design of new coumarin dyes

having thiophene moieties for highly efficient organic-dye-sensitized solar cells. New J Chem 27:783–785
24. Mishra A, Fischer MKR, Bauerle P (2009) Metal-free organic dyes for dye-sensitized solar cells: from structure: property relationships to design rules. Angew Chem Int Ed 48:2474–2499
25. De Angelis F, Fantacci S, Selloni A (2004) Time-dependent density functional theory study of the absorption spectrum of [Ru(4,4′-COOH-2,2′-bpy)2(NCS)2] in water solution: influence of the pH. Chem Phys Lett 389:204–208
26. De Angelis F, Fantacci S, Selloni A, Nazeeruddin MK (2005) Time dependent density functional theory study of the absorption spectrum of the [Ru(4,4′-COO−-2,2′-bpy)2(X)2]4− (X = NCS, Cl) dyes in water solution. Chem Phys Lett 415:115–120
27. Xu Y, Chen WK, Cao MJ, Liu SH, Li JQ, Philippopoulos AI, Falaras P (2006) A TD-DFT study on the electronic spectrum of Ru(II)L2 [L = bis(5′-methyl-2,2′-bipyridine-6-carboxylato)] in the gas phase and DMF solution. Chem Phys 330:204–211
28. Ito S, Zakeeruddin SM, Humphry-Baker R, Liska P, Charvet R, Comte P, Nazeeruddin MK, Péchy P, Takata M, Miura H, Uchida S, Grätzel M (2006) High-efficiency organic-dye- sensitized solar cells controlled by nanocrystalline-TiO_2 electrode thickness. Adv Mater 18:1202–1205
29. De Angelis F, Fantacci S, Selloni A, Grätzel M, Nazeeruddin MK (2007) Influence of the sensitizer adsorption mode on the open-circuit potential of dye-sensitized solar cells. Nano Lett 7:3189–3195
30. De Angelis F, Fantacci S, Selloni A, Nazeeruddin MK, Grätzel M (2007) Time-dependent density functional theory investigations on the excited states of Ru(II)-dye-sensitized TiO2 nanoparticles: the role of sensitizer protonation. J Am Chem Soc 129:14156–14157
31. De Angelis F, Fntacci S, Selloni A (2008) Alignment of the dye's molecular levels with the TiO_2 band edges in dye-sensitized solar cells: a DFT–TDDFT study. Nanotechnology 19:424002–424009
32. Di Censo D, Fantacci S, De Angelis F, Klein C, Evans N, Kalyanasundaram K, Bolink HJ, Grätzel M, Nazeeruddin MK (2008) Synthesis, characterization, and DFT/TD-DFT calculations of highly phosphorescent blue light-emitting anionic iridium complexes. Inorg Chem 47:980–989
33. Kurashige Y, Nakajima T, Kurashige S, Hirao K, Nishikitani Y (2007) Theoretical investigation of the excited states of coumarin dyes for dye-sensitized solar cells. J Phys Chem A 111:5544–5548
34. Balanay MP, Kim DH (2008) DFT/TD-DFT molecular design of porphyrin analogues for use in dye-sensitized solar cells. Phys Chem Chem Phys 10:5121–5127
35. Satoh N, Cho JS, Higuchi M, Yamamoto K (2003) Novel triarylamine dendrimers as a hole-transport material with a controlled metal-assembling function. J Am Chem Soc 125:8104–8105
36. Satoh N, Nakashima T, Yamamoto K (2005) Metal-assembling dendrimers with a triarylamine core and their application to a dye-sensitized solar cell. J Am Chem Soc 127:13030–13038
37. Wang Q, Zakeeruddin SM, Cremer J, Bäuerle P, Humphry-Baker R, Gratzel M (2005) Cross surface ambipolar charge percolation in molecular triads on mesoscopic oxide films. J Am Chem Soc 127:5706–5713
38. Al-Sehemi AG, Irfan A, Asiri AM, Ammar YA (2012) Synthesis, characterization and DFT study of methoxybenzylidene containing chromophores for DSSC materials. Spectrochimica Acta Part A. doi:10.1016/j.saa.2012.01.016
39. Al-Sehemi AG, Irfan A (2012) Dye-Sensitized nanocrystalline TiO_2 solar cell: toward high sun light to electricity conversion (submitted)
40. Stein T, Kronik L, Baer R (2009) Prediction of charge-transfer excitations in coumarin-based dyes using a range-separated functional tuned from first principles. J Chem Phys 131:244119–244123
41. Wong BM, Piacenza M, Sala FD (2009) Absorption and fluorescence properties of oligothiophene biomarkers from long-range-corrected time-dependent density functional theory. Phys Chem Chem Phys 11:4498–4508
42. Wong BM, Cordaro JG (2008) Coumarin dyes for dye-sensitized solar cells: a long-range-corrected density functional study. J Chem Phys 129:214703–214710
43. Lange AW, Rohrdanz MA, Herbert JM (2008) Charge-transfer excited states in a π-stacked adenine dimer, as predicted using long-range-corrected time-dependent density functional theory. J Phys Chem B 112:6304–6308
44. Rohrdanz MA, Herbert JM (2008) Simultaneous benchmarking of ground- and excited-state properties with long-range-corrected density functional theory. J Chem Phys 129:034107–034115
45. Toulouse J, Colonna F, Savin A (2005) Short-range exchange and correlation energy density functionals: beyond the local-density approximation. J Chem Phys 122:014110–014119
46. Livshits E, Baer R (2007) A well-tempered density functional theory of electrons in molecules. Phys Chem Chem Phys 9:2932–2941
47. Preat J (2010) Photoinduced energy-transfer and electron-transfer processes in dye-sensitized solar cells: TDDFT insights for triphenylamine dyes. J Phys Chem C 114:16716–16725
48. Preat J, Michaux C, Jacquemin D, Perpète EA (2009) Enhanced efficiency of organic dye-sensitized solar cells: Triphenylamine derivatives. J Phys Chem C 113:16821–16833
49. Magyar RJ, Tretiak S (2007) Dependence of spurious charge-transfer excited states on orbital exchange in TDDFT: large molecules and clusters. J Chem Theory Comput 3:976–987
50. Irfan A, Al-Sehemi AG (2012) Donor-bridge-acceptor effect on the electron injection in triphenylamine based sensitizers: density functional theory investigations (submitted)
51. Irfan A, Al-Sehemi AG (2012) Quantum chemical investigations of the electron injection in triphenylamine based sensitizers (submitted)
52. Peach MJG, Benfield P, Helgaker T, Tozer DJ (2008) Excitation energies in density functional theory: an evaluation and a diagnostic test. J Chem Phys 128:044118
53. Bertolino CA, Ferrari AM, Barolo C, Viscardi G, Caputo S, Coluccia G (2006) Solvent effect on indocyanine dyes: a computational approach. Chem Phys 330:52–59
54. Jacquemin D, Perpète EA, Scalmani G, Frisch MJ, Kobayashi R, Adamo C (2007) Assessment of the efficiency of long-range corrected functionals for some properties of large compounds. J Chem Phys 126:144105
55. Guillaumont D, Nakamura S (2000) Calculation of the absorption wavelength of dyes using time-dependent density-functional theory (TD-DFT). Dyes Pigment 46:85–92
56. Becke AD (1993) Density-functional thermochemistry. III. The role of exact exchange. J Chem Phys 98:5648–5652
57. Lee C, Yang W, Parr RG (1988) Development of the Colle-Salvetti correlation-energy formula into a functional of the electron density. Phys Rev B 37:785–789
58. Stephens PJ, Devlin FJ, Chabalowski CF, Frisch MJ (1994) Ab initio calculation of vibrational absorption and circular dichroism spectra using density functional force fields. J Phys Chem 98:11623–11627
59. Lynch BJ, Fast PL, Harris M, Truhlar DG (2000) Adiabatic connection for kinetics. J Phys Chem A 104:4811–4815
60. Perdew JP, Chevary JA, Vosko SH, Jackson KA, Pederson MR, Singh DJ, Fiolhais C (1992) Atoms, molecules, solids, and surfaces: applications of the generalized gradient approximation for exchange and correlation. Phys Rev B 46:6671–6687

61. Walsh PJ, Gordon KC, Officer DL, Campbell WM (2006) A DFT study of the optical properties of substituted Zn(II)TPP complexes. J Mol Struct THEOCHEM 759:17–24
62. Cleland DM, Gordon KC, Officer DL, Wagner P, Walsh PJ (2009) Tuning the optical properties of ZnTPP using carbonyl ring fusion. Spectrochimica Acta Part A 74:931–935
63. Zhang CR, Liang WZ, Chen HS, Chen YH, Wei ZQ, Wu YZ (2008) Theoretical studies on the geometrical and electronic structures of N-methyle-3,4-fulleropyrrolidine. J Mol Struct THEOCHEM 862:98–104
64. Sun J, Song J, Zhao Y, Liang WZ (2007) Real-time propagation of the reduced one-electron density matrix in atom-centered Gaussian orbitals: application to absorption spectra of silicon clusters. J Chem Phys 127:234107–234113
65. Matthews D, Infelta P, Grätzel M (1996) Calculation of the photocurrent-potential characteristic for regenerative, sensitized semiconductor electrodes. Sol Energy Mater Sol Cells 44:119–155
66. Frisch MJ, et al. (2009) Gaussian 09, revision A.1. Gaussian, Inc., Wallingford
67. Cossi M, Barone V (2001) Time-dependent density functional theory for molecules in liquid solutions. J Chem Phys 115:4708–4717
68. Amovilli C, Barone V, Cammi R, Cancès E, Cossi M, Mennucci B, Pomelli CS, Tomasi J (1998) Recent advances in the description of solvent effects with the polarizable continuum model. Adv Quantum Chem 32:227–261
69. Tomasi J, Mennucci B, Cammi R (2005) Quantum mechanical continuum solvation models. Chem Rev 105:2999–3094
70. Preat J, Jacquemin D, Perpete E (2010) Design of new triphenylamine-sensitized solar cells: a theoretical approach. Environ Sci Technol 44:5666–5671
71. Preat J (2010) Photoinduced energy-transfer and electron-transfer processes in dye-sensitized solar cells: TDDFT insights for triphenylamine dyes. Sol Energy Mater Sol Cells 114:16716–16725
72. Pourtois G, Beljonne J, Ratner MA, Bredas JL (2002) Photoinduced electron-transfer processes along molecular wires based on phenylenevinylene oligomers: a quantum-chemical insight. J Am Chem Soc 124:4436–4447
73. Hsu C (2009) The electronic couplings in electron transfer and excitation energy transfer. Acc Chem Res 42:509–518
74. Marcus RA (1993) Electron transfer reactions in chemistry. Theory and experiment. Rev Mod Phys 65:599–610
75. Asbury JB, Wang YQ, Hao E, Ghosh H, Lian T (2001) Evidences of hot excited state electron injection from sensitizer molecules to TiO_2 nanocrystalline thin films. Res Chem Intermed 27:393–406
76. Katoh R, Furube A, Yoshihara T, Hara K, Fujihashi G, Takano S, Murata S, Arakawa H, Tachiya M (2004) Efficiencies of electron injection from excited N3 dye into nanocrystalline semiconductor (ZrO_2, TiO_2, ZnO, Nb_2O_5, SnO_2, In_2O_3) films. J Phys Chem B 108:4818–4822
77. Hagfeldt A, Grätzel M (1995) Light-induced redox reactions in nanocrystalline systems. Chem Rev 95:49–68
78. Barbara PF, Meyer TJ, Ratner MA (1996) Contemporary issues in electron transfer research. J Phys Chem 100:13148–13168
79. Nalwa HS (2001) Handbook of advanced electronic and photonic materials and devices. Academic, San Diego
80. Cassida M (1995) Recent advances in density functional methods: time dependent density functional response theory for molecules; DP Chong, Singapore
81. Harris DC, Bertolucci MD (1998) Symmetry and spectroscopy. Dover, New York
82. Liu D, Fessenden RW, Hug GL, Kamat PV (1997) Dye capped semiconductor nanoclusters. Role of back electron transfer in the photosensitization of SnO_2 nanocrystallites with cresyl violet aggregates. J Phys Chem B 101:2583–2590
83. Ning Z, Zhang Q, Wu W, Pei H, Liu B, Tian H (2008) Starburst triarylamine based dyes for efficient dye-sensitized solar cells. J Org Chem 73:3791–3797